Sheffield Hallam University

Vehicle sideslip estimation for four-wheel-steering vehicles using a particle filter

LENZO, Basilio <http://orcid.org/0000-0002-8520-7953> and DE CASTRO, Ricardo

Available from Sheffield Hallam University Research Archive (SHURA) at:

http://shura.shu.ac.uk/24916/

Published version

Copyright and re-use policy

Sheffield Hallam University Research Archive
http://shura.shu.ac.uk

Vehicle sideslip estimation for four-wheel-steering vehicles using a particle filter

Basilio Lenzo[1][0000-0002-8520-7953] and Ricardo De Castro[2][0000-0002-5546-3999]

[1]Sheffield Vehicle Dynamics Research group, Department of Engineering and Mathematics, Sheffield Hallam University, Sheffield S11WB, United Kingdom
[2]Institute of System Dynamics and Control, German Aerospace Center (DLR), Weßling D-82234, Germany
basilio.lenzo@shu.ac.uk

Abstract. The availability of the most relevant vehicle states is crucial for the development of advanced vehicle control systems and driver assistance systems. Specifically the vehicle sideslip angle plays a key role, yet this state is unpractical to measure and still not straightforward to estimate. This paper investigates a particle filter approach to estimate the chassis sideslip angle of road vehicles. The filter relies on a physical model of the vehicle and on measurements available from cheap and widespread sensors including inertial measurement unit and steering wheel angle sensor(s). The approach is validated using experimental data collected with the research platform RoboMobil (RoMo), a by-wire electric vehicle with wheel-individual traction and steering actuators. Results show that the performance of the proposed particle filter is satisfactory, and indicate directions for further improvement.

Keywords: Sideslip angle, particle filter, electric vehicles, estimation, rear wheel steering, experiments.

List of symbols

a_y vehicle lateral acceleration (m/s^2)
a_y^* vehicle lateral acceleration with roll angle correction (m/s^2)
C_{y1} cornering stiffness of the front axle (N/rad)
C_{y2} cornering stiffness of the rear axle (N/rad)
c input vector
e_i difference in measurement between actual one and i-th particle prediction
F_{x1} longitudinal force at front axle (N)
F_{x2} longitudinal force at rear axle (N)
F_{y1} lateral force at front axle (N)
F_{y2} lateral force at rear axle (N)
$F_{z1,0}$ static vertical load on front axle (N)
$F_{z2,0}$ static vertical load on rear axle (N)
f function describing the model propagation

g gravity acceleration (m/s^2)

h function relating the measurements to the state vector x

J_z vehicle yaw mass moment of inertia (kg m^2)

k time step

m vehicle mass (kg)

N number of samples

n_p number of particles of the particle filter

n_x process noise

n_y measurement noise

q exogenous input vector

r vehicle yaw rate (rad/s)

u vehicle longitudinal velocity (m/s)

v vehicle lateral velocity (m/s)

W_{a_y} weight on the lateral acceleration error

W_i weight for the i-th particle

W_r weight on the yaw rate error

w_1 front semi-wheelbase (m)

w_2 rear semi-wheelbase (m)

x state vector

$\hat{x}$ estimated state vector

y measurement vector

α_1 front tire slip angle (rad)

α_2 rear tire slip angle (rad)

β sideslip angle at the centre of mass (rad)

$\hat{\beta}$ estimated sideslip angle at the centre of mass (rad)

β_1 front sideslip angle (rad)

β_2 rear sideslip angle (rad)

Δt time step (s)

δ_1 front steering angle (rad)

δ_2 rear steering angle (rad)

φ estimated roll angle (rad)

μ average tire-road friction coefficient

ϕ_i predicted measurement for i-th particle

χ_i i-th particle

1 Introduction

In recent years, industrial and academic research has dedicated great effort to the development of advanced driver assistance systems [1]. These systems use a combination of environmental perception, estimation and control methods to assist the driver manoeuvring the vehicle - in both normal and challenging driving conditions - improving comfort and road safety. However, to guarantee correct operation of these systems, accurate knowledge of vehicle states and parameters is required. Variables such as the vehicle sideslip angle (from a top view, the angle between the vehicle

longitudinal axis and the centre of mass velocity vector) or the tyre-road friction coefficient are of paramount importance, especially from the point of view of lateral dynamics control [2]. In practice, such variables are difficult, expensive or even impossible to be directly measured. That encourages the use of estimation techniques.

In the literature, several types of estimation methods can be found, including model-based (e.g. Kalman Filters) [3-4] and AI-based (e.g. neural networks) methods [3]. The main issue of AI-based methods is that their performance might deteriorate when vehicle operation conditions diverge from the ones used in training data [5]. One of the main issues of model-based approaches is that they need a sufficiently accurate tyre model. This accurate model is difficult to obtain in practice, because tyre behaviour is subject to changes with, e.g., wear, road conditions, temperature etc. To tackle this issue, some authors proposed estimation approaches where vehicle states and model parameters are simultaneously estimated [6-7]. Another approach, investigated in [8], exploits kinematic models to estimate vehicle states, which are less sensitive to parameter uncertainties. However, these methods are affected by measurement noise and sensor drift, which requires several expedients to make these methods reliable (see patent [9] for details).

In this paper, a particle filter (PF) approach is investigated to estimate the vehicle sideslip angle. The particle filter has the advantage of being a very general and flexible estimation framework [10]. Kalman Filters, instead, come with several simplifying hypotheses, such as no correlation between process and measurement noise and Gaussian disturbances. The herein developed particle filter relies on a physical model of the vehicle and on measures available from cheap and widespread sensors such as inertial measurement unit (IMU) and steering wheel angle sensor(s). It is also designed having in mind vehicles with four-wheel steering.

The remainder of the paper is structured as follows. Section 2 describes the vehicle model and the experimental platform. The design of the particle filter is discussed in Section 3. Results are presented in Section 4. Conclusions are in Section 5.

2 Vehicle model

The particle filter is designed based on a non-linear single track model (Fig. 1, left). Differently from a classical single track vehicle model, rear steering is herein considered - that is a feature of the experimental vehicle used for the validation of the algorithm. That is the research platform RoboMobil (RoMo, Fig. 1, right) - a by-wire electric vehicle with wheel-individual traction and steering actuators - built by the DLR for demonstrating the benefits of transferring advanced space and robotics technologies to electric road vehicles (see [11] for details).

The Adapted ISO sign convention is adopted in this work [12]. The three sets of equations describing this non-linear single track model can be written as follows.

Equilibrium equations

$$ma_y^* = m(\dot{v} + ur) = F_{x1} \sin \delta_1 + F_{y1} \cos \delta_1 + F_{x2} \sin \delta_2 + F_{y2} \cos \delta_2 \tag{1a}$$

$$J_z \dot{r} = \left(F_{x1} \sin \delta_1 + F_{y1} \cos \delta_1\right)w_1 - (F_{x2} \sin \delta_2 + F_{y2} \cos \delta_2)w_2 \tag{1b}$$

Congruence equations

$$\alpha_1 = \delta_1 - \beta_1 = \delta_1 - \tan^{-1}\frac{v+rw_1}{u} \tag{2a}$$

$$\alpha_2 = \delta_2 - \beta_2 = \delta_2 - \tan^{-1}\frac{v-rw_2}{u} \tag{2b}$$

Constitutive equations

$$F_{yi} = \begin{cases} C_{yi}\alpha_i & if \ |\alpha_i| \leq \frac{\mu F_{zi,0}}{C_{yi}} \\ \mu F_{zi,0} & otherwise \end{cases} \tag{3}$$

for $i = 1,2$, where the static loads at the front and rear axle are $F_{z1,0} = \frac{mgw_2}{w_1+w_2}$ and $F_{z2,0} = \frac{mgw_1}{w_1+w_2}$, respectively. For a detailed description of the variables and parameters used in the above mathematical model, the reader is referred to the List of Symbols.
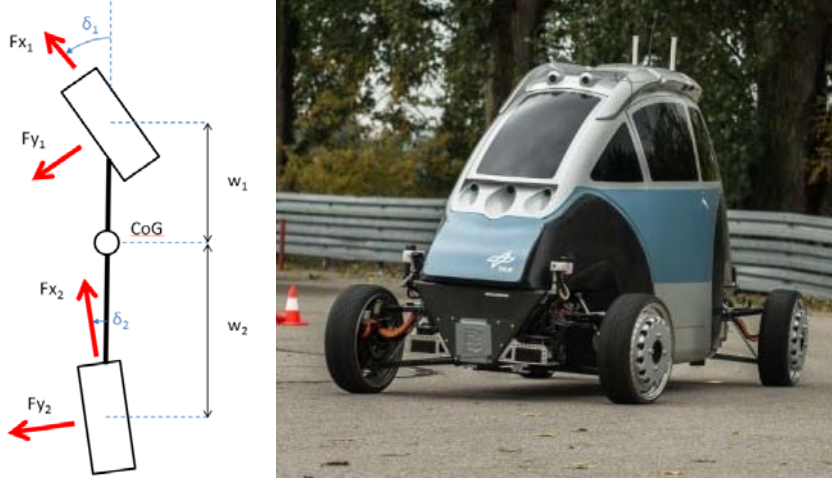

Fig.1. (left) Single track vehicle model with rear steering capability; (right) The RoMo vehicle, developed at the German Aerospace Center (DLR).

In this work, only lateral dynamics is considered. We assume that the longitudinal velocity (u) and the longitudinal forces (F_{x1}, F_{x2}) are available. For example, the longitudinal forces F_{x1} and F_{x2} can be obtained based on the torque demands at each motor, while the longitudinal velocity can be inferred using wheel speed sensors (assuming longitudinal tyre slips are low).

The continuous-time equations (1)-(3) are converted into discrete-time through Euler's method [13]. The vehicle state includes the vehicle lateral velocity (v) and yaw rate (r). Thus, (1)-(3) are rearranged to obtain expressions of the vector field $(\dot{v} \quad \dot{r})^T$, leading to the following discrete-time vehicle model:

$$x(k + 1) = f(x(k), c(k), q(k)) + n_x \tag{4a}$$

$$y(k) = h(x(k), c(k), q(k)) + n_y \tag{4b}$$

The vehicle state is $x = (v \quad r)^T$, the measurement vector is $y = (a_y^* \quad r)^T$, the input vector is $c = (\delta_1 \quad \delta_2)^T$, the exogenous input vector is $q = (u, F_{x1}, F_{x2})$, n_x and n_y are, respectively, the process noise and the measurement noise. The (noise-free) relationship between measurement vector and state vector is: $a_y^* = 1/m(F_{x1} \sin \delta_1 + F_{y1} \cos \delta_1 + F_{x2} \sin \delta_2 + F_{y2} \cos \delta_2)$ and, trivially, $r = r$. Based on this framework, the goal of the filter is to estimate x.

3 Particle filter design

The PF is a recursive Bayesian estimator based on Monte-Carlo simulations [14]. Multiple potential representations of the state, denoted as particles, are propagated, weighted and resampled at each time step. Large numbers of particles are normally required, resulting in significant computational burden. PFs have gained popularity recently, due to the improved processing power capabilities of modern computers. The workflow of the developed particle filter can be described as follows (Fig. 2):

1. the particle filter is initialised; that includes the selection of the number of particles (n_p), their initial state and their covariance: the particles are initially randomly picked from a normal distribution with mean at initial state and appropriate covariance distribution around the initial state, $\chi_1(k), \chi_2(k), \ldots, \chi_{n_p}(k)$;
2. based on the vehicle model (prediction model, Equation 4a), each particle evolves into a new state, $\chi_i(k+1) = f(\chi_i(k), c(k), q(k))$;
3. for each of the particles, the corresponding predicted measurements are computed, $\phi_i(k) = h(\chi_i(k), c(k), q(k))$;
4. the predicted measurements are compared to the actual ones, and an error vector is calculated, $e_i(k) = y(k) - \phi_i(k)$;
5. the measurement likelihood function $\text{MLF}(e_i(k))$ is calculated for each particle;
6. the best estimate of the state is calculated based on the measurement prediction and the likelihood; $\hat{x}(k) = \sum_i W_i \chi_i(k)$, weighted by the likelihood function: $W_i = \text{MLF}(e_i(k)) / \sum_j \text{MLF}(e_j(k))$;
7. the particles are resampled around the recent best estimate of the state [15].

The measurement likelihood function adopted in this work was inspired by [14], which considers a bell curve. Accordingly, for each particle i, the MLF is defined as

$$MLF(e_i) = e^{-(e_i^T W_e e_i)} \tag{5}$$

where $W_e = diag(W_{a_y}, W_r)$ is a diagonal weight matrix tuned by the designer.

Appropriate phase-lag-free filters [16] were applied to the measured quantities (yaw rate, longitudinal acceleration, lateral acceleration etc.) in order to attenuate the effect of measurement noise – see, e.g., Fig. 5d. Additionally, the measured lateral acceleration was corrected based on an estimate of the vehicle roll angle, similarly to [17] (since only the lateral dynamics is considered in the estimation, pitch compensation is neglected):

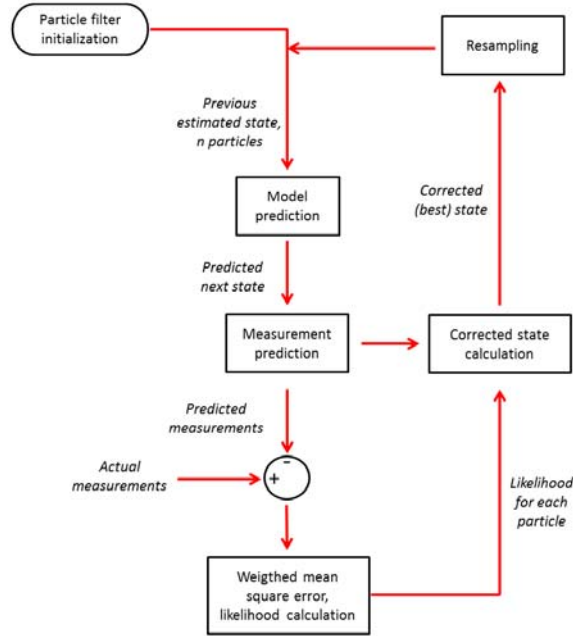$$a_y^* = \frac{a_y}{\cos \varphi} - g \tan \varphi \tag{6}$$

Fig.2. Particle filter workflow.

The estimated vehicle sideslip angle was finally computed as $\hat{\beta} = \tan^{-1}\frac{v}{u}$.

4 Experimental Validation

This section presents a selection of results discussing the performance of the developed particle filter. The test data was obtained based on several manoeuvres performed with the ROMO over dry tarmac ($\mu \approx 1$), including: i) sinusoidal steering excitation; ii) sine sweep steering excitation; iii) quasi-steady-state cornering, and iv) quasi-steady-state cornering with sudden braking. The actual vehicle states were collected using an advanced inertial measurement unit (OXTS RT4003) and an optical sensor (Correvit L-350), sampled at 4 ms. The PF estimator described in Section 3 was implemented in Matlab environment with a default number of particles set to $n_p = 100$.

Fig. 3 depicts the results of the sinusoidal steering input manoeuvre, including the time history of the steering angles. Fig. 4 shows the PF performance with the sine sweep (Fig. 4a) and the quasi-steady-state cornering manoeuvre (Fig. 4b). The manoeuvres shown in Fig. 3 and Fig. 4 are all with medium values of lateral acceleration (up to 6 m/s^2). Inspecting the obtained results, one can find a very good agreement between the actual and estimated sideslip angle in both dynamic and quasi-stationary manoeuvres.
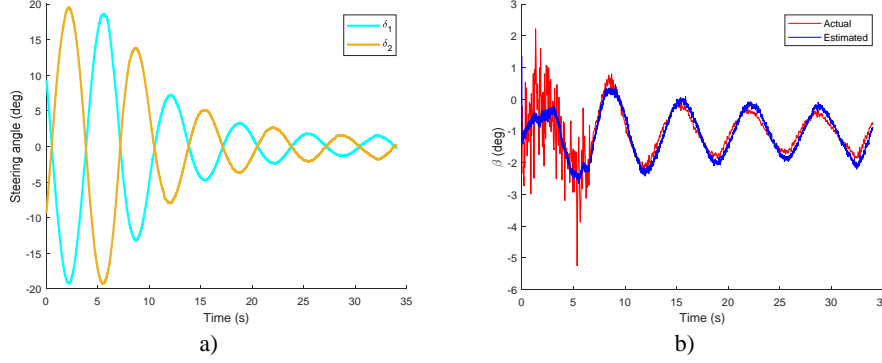
Fig.3. Experimental validation on a sinusoidal steering input manoeuvre with linearly increasing speed (up to $u = 14$ m/s): (a) steering angles; (b) sideslip angle and PF estimation ($n_p = 100$).
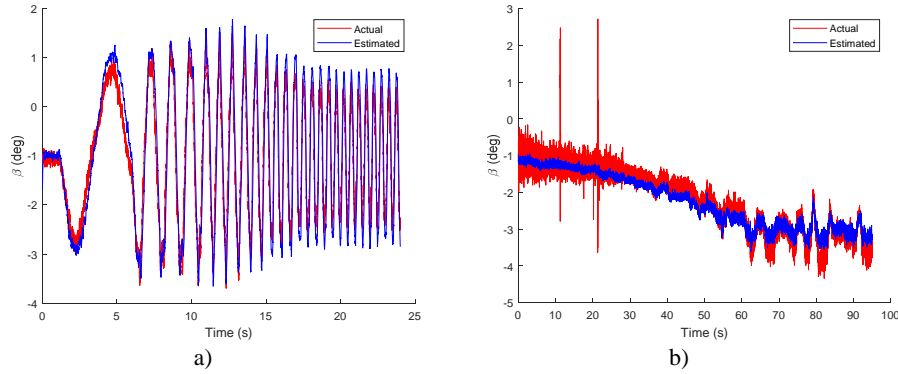

Fig.4. Experimental validation of the PF estimation ($n_p = 100$) on: (a) Sine sweep ($u = 15$ m/s); (b) Quasi-steady-state cornering manoeuvre, 30 m radius.

Despite these good estimation results, the PF parameterisation evaluated in Fig. 3 and Fig. 4 employed a large number of particles, which requires high computation effort. To mitigate this issue, and find a good balance between estimation performance and computational cost, the PF was evaluated with different numbers of particles. The performance of the filter was assessed through the root mean square error ($RMSE$) of the sideslip angle:

$$RMSE = \sqrt{\frac{\sum_{k=1}^{N}\left(\beta(k) - \hat{\beta}(k)\right)^2}{N}} \tag{7}$$

while the PF's computational times were obtained on a desktop computer, with 3.40 GHz processor and 8 GB RAM.

Fig. 5 shows the effect of different numbers of particles (i.e. 10, 100, 1000) during a challenging quasi-steady-state cornering manoeuvre, where the lateral acceleration is increased from 0 up to around 9 m/s², followed by a sudden braking action. Gener-

ally, all PF parameterisations produce satisfactory estimations of the sideslip angle, with errors smaller than 0.5 deg. The only exception is the estimation around 15-16s, when the brake is engaged (Fig. 5d). The likely cause for the estimation divergence might be neglected pitch effects in the estimation model. This is to be addressed in future work. A more comprehensive evaluation of the PF parameterisations is shown in Table 1, which contains the computational cost and RMSE performance of the PF for different numbers of particles and manoeuvres. One can find that, decreasing the number of particles from 1000 to 100 leads to a significant reduction in the PF's computational effort (up to 8x times reduction), while having an almost negligible impact in the RMSE performance. Decreasing the number of particles to 10 allows another 2-3 times reduction in computational effort. In fact, since the PF execution time for $n_p = 10$ is inferior to the maneuver(s) duration(s), this PF parameterisation might be suitable for real-time implementation. However, this PF parameterisation also degrades the estimation performance. In comparison with the case $n_p = 1000$, the PF with $n_p = 10$ increases the sideslip angle RMSE by 4.4% for the sine sweep manoeuvre (best estimation performance) and by 53% for the quasi-steady-state cornering with sudden braking (worst estimation performance).
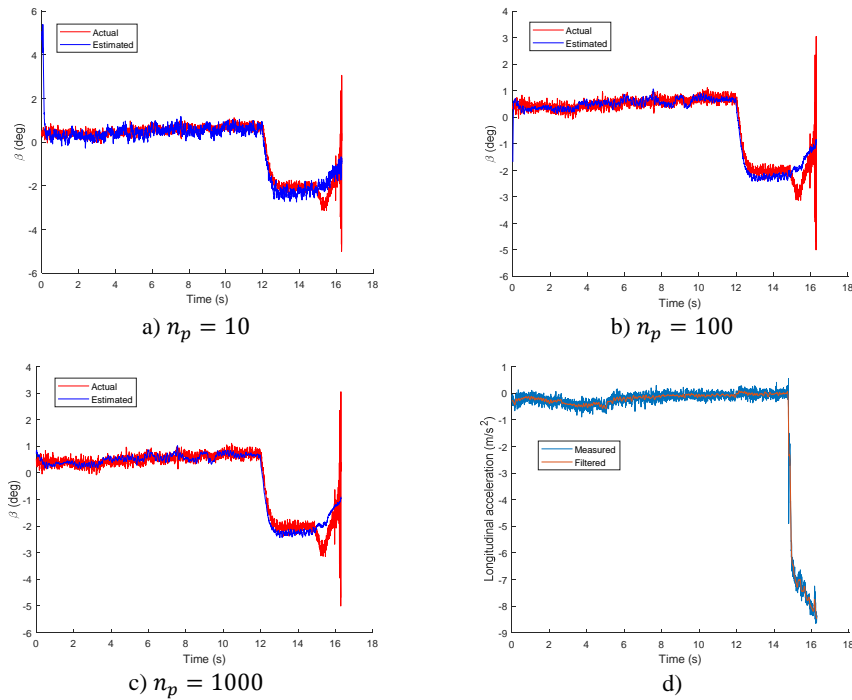

a) $n_p = 10$

b) $n_p = 100$

c) $n_p = 1000$

d)

Fig.5. Quasi-steady-state cornering and sudden braking manoeuvre, radius 30 m: Particle filter with (a) 10 particles; (b) 100 particles; (c) 1000 particles; (d) Longitudinal acceleration.

Analysing in more detail the time domain results of the PF with $n_p = 10$ (Fig. 5a) and with $n_p = 1000$ (Fig. 5c) reveals that: i) both PF variants have similar average estimation behaviour; ii) the PF with lower number of particles has higher estimation variance (i.e. noise). These results highlight the trade-offs between computational effort vs estimation variance that the designer will face during the practical commissioning of PF-based vehicle estimators.

Table 1. Computational cost and performance comparison.

Test	Number of particles	Manoeuvre duration (s)	PF running time (s)	RMSE (deg)
Sinusoidal steering input	10	34	28.9	0.49
	100		88.4	0.41
	1000		601	0.41
Sine sweep	10	24	19.2	0.48
	100		49.6	0.46
	1000		315	0.46
Quasi-steady-state cornering	10	95	94.2	0.33
	100		502.6	0.28
	1000		4256.6	0.26
Quasi-steady-state cornering and sudden braking	10	16.3	13.2	0.49
	100		29.1	0.33
	1000		155.5	0.32

5 Conclusions

This paper presented a particle filter method for estimation of the vehicle sideslip angle based on a non-linear single track vehicle model with rear steering capability.
The algorithm was shown effective on a number of experimental manoeuvres performed with the DLR's robotic platform RoMo. The sensitivity analysis also revealed that the computational effort of the particle filter can be significantly reduced by decreasing the number of particles, but at the expense of higher estimation variance.

Future work will tackle: i) the implementation of an effective strategy for the estimation of the vehicle longitudinal velocity; ii) the adoption of a double track vehicle model and a more sophisticated tyre model; iii) the implementation of roll and pitch dynamics; iv) the investigation of computational efficient approaches for a real-time applicability of the method while preserving performance.

6 Acknowledgements

References

1. Gordon, T., Howell, M., Brandao, F., Integrated control methodologies for road vehicles, Vehicle System Dynamics, 40(1-3), pp. 157-190 (2003).
2. Tota, A., Lenzo, B., Lu, Q, et al., On the experimental analysis of integral sliding modes for yaw rate and sideslip control of an electric vehicle with multiple motors, International Journal of Automotive Technology, 19(5), pp. 811-823 (2018).
3. Chindamo, D., Lenzo, B., Gadola, M., On the Vehicle Sideslip Angle Estimation: A Literature Review of Methods, Models, and Innovations, Applied Sciences, 8(3), 355 (2018).
4. Pieralice, C., Lenzo, B., Bucchi, F. and Gabiccini, M., Vehicle sideslip angle estimation using Kalman filters: modelling and validation, The International Conference of IFToMM Italy, pp. 114-122, Springer (2018).
5. Melzi, S. and Sabbioni, E., On the vehicle sideslip angle estimation through neural networks: Numerical and experimental results. Mechanical Systems and Signal Processing, 25(6), pp. 2005-2019 (2011).
6. Cheli, F., Sabbioni, E., Pesce, M., Melzi, S., A methodology for vehicle sideslip angle identification: comparison with experimental data. Vehicle System Dynamics, 45(6), pp. 549-563 (2007).
7. Van Aalst, S., Naets, F., Boulkroune, B., De Nijs, W., Desmet, W., An Adaptive Vehicle Sideslip Estimator for Reliable Estimation in Low and High Excitation Driving, 15th IFAC Symposium on Control in Transportation Systems (CTS 2018), Savona, Italy (2018).
8. Selmanaj, D., Corno, M., Panzani, G., Savaresi, S.M., Vehicle sideslip estimation: A kinematic based approach. Control Engineering Practice, 67, pp.1-12 (2017).
9. Savaresi, S., Corno, M., Selmanaj, et al., Method For Estimating A Vehicle Side Slip Angle, Computer Program Implementing Said Method, Control Unit Having Said Computer Program Loaded, And Vehicle Comprising Said Control Unit, US20170247038A1 (2017).
10. György, K., Kelemen, A., Dávid, L. Unscented Kalman filters and Particle Filter methods for nonlinear state estimation. Procedia Technology, 12, pp. 65-74 (2014).
11. Brembeck, J., Ho, L. M., Schaub, A., Satzger, C., Tobolar, J., Bals, J., Hirzinger, G., Romo-the robotic electric vehicle (2011).
12. Pacejka, H.B., Tyre and vehicle dynamics, Butterworth-Heinemann (2006).
13. Koenig, H., Modern computational methods. CRC Press (1998).
14. Bogdanski, K. and Best, M.C., Kalman and particle filtering methods for full vehicle and tyre identification. Vehicle System Dynamics, 56(5), pp.769-790 (2018).
15. Douc, R. and Cappé, O., Comparison of resampling schemes for particle filtering. In ISPA 2005. Proceedings of the 4th International Symposium on Image and Signal Processing and Analysis, pp. 64-69 (2005).
16. Lenzo, B., Bucchi, F., Sorniotti, A. and Frendo, F., On the handling performance of a vehicle with different front-to-rear wheel torque distributions. Vehicle System Dynamics, 57:11, pp. 1685-1704 (2019).
17. Grip, H.F., Imsland, L., Johansen, T.A., Kalkkuhl, J.C. and Suissa, A., Vehicle sideslip estimation. IEEE control systems magazine, 29(5), pp.36-52 (2009).